

Supermassive black hole spin-flip during the inspiral

László Á. Gergely^{1,2*}, Peter L. Biermann^{3,4,5,6,7†}, Laurențiu I. Caramete^{8‡}

¹ Department of Theoretical Physics, University of Szeged, Hungary

² Department of Experimental Physics, University of Szeged, Hungary

³ MPI for Radioastronomy, Bonn, Germany

⁴ Department of Physics & Astronomy, University of Bonn, Germany

⁵ Department of Physics & Astronomy, University of Alabama, Tuscaloosa, AL, USA

⁶ Department of Physics, University of Alabama at Huntsville, AL, USA

⁷ FZ Karlsruhe, and Physics Department, University of Karlsruhe, Germany

⁸ Institute for Space Sciences, Bucharest, Romania

* gergely@physx.u-szeged.hu; † plbiermann@mpifr-bonn.mpg.de; ‡ lcaramete@gmail.com

Abstract. During post-Newtonian evolution of a compact binary, a mass ratio ν different from 1 provides a second small parameter, which can lead to unexpected results. We present a *statistics of supermassive black hole candidates*, which enables us first to derive their mass distribution, then to establish a logarithmically even probability in ν of the mass ratios at their encounter. In the mass ratio range $\nu \in (1/30, 1/3)$ of supermassive black hole mergers representing 40% of all possible cases, the combined effect of spin-orbit precession and gravitational radiation leads to a spin-flip of the dominant spin during the *inspiral* phase of the merger. This provides a mechanism for explaining a large set of observations on X-shaped radio galaxies. In another 40% with mass ratios $\nu \in (1/30, 1/1000)$ a spin-flip never occurs, while in the remaining 20% of mergers with mass ratios $\nu \in (1/3, 1)$ it may occur during the plunge. We analyze the magnitude of the spin-flip angle occurring during the inspiral as function of the mass ratio and original relative orientation of the spin and orbital angular momentum. We also derive a formula for the *final spin* at the end of the inspiral in this mass ratio range.

1. Introduction

During galaxy mergers, following a regime of slow approach due to dynamical friction, eventually the central supermassive black holes (SMBHs) approach each other to a separation of the order of 10^3 Schwarzschild radii, when gravitational radiation takes over as the leading order dissipative effect. The Laser Interferometer Space Antenna (LISA, see [1]) is expected to detect merging binary SMBHs with masses $m_1 + m_2 \leq 10^7$ solar masses (M_\odot) up to redshift $z \approx 30$. A post-Newtonian approach is well suited to describe their forthcoming *inspiral*, a regime we define in terms of the post-Newtonian (PN) parameter $\varepsilon = Gm/c^2 r \approx v^2/c^2 \in (\varepsilon_{in} = 10^{-3}, \varepsilon_{fin} = 10^{-1})$, where r and v characterize the orbital separation (from the center of mass) and speed of the reduced mass particle, G is the gravitational constant and c the speed of light. Various corrections to the conservative dynamics add up to 2 PN, while the gravitational radiation results in dissipation of energy, angular momentum and orbital angular momentum at 2.5 PN.

The leading order conservative correction to the Newtonian dynamics in a compact binary, which results in a change of the orbital plane (defined by the direction $\hat{\mathbf{L}}_N$ of the Newtonian orbital angular momentum $\mathbf{L}_N = \mu \mathbf{r} \times \mathbf{v}$ of the reduced mass particle μ) is the spin-orbit (SO) interaction [2], [3]. The precessional time-scale (the time during which the normal to the orbit $\hat{\mathbf{L}}_N$ undergoes a full rotation) is longer than the orbital period, however shorter than the characteristic time-scale of gravitational radiation (defined as L/\dot{L} , where L is the magnitude of the total orbital angular momentum). Combined with the leading order gravitational radiation backreaction averaged over one quasicircular orbit, the SO correction provides a fair approximation to orbital dynamics, explored in Refs. [3], [4].

X-shaped radio galaxies (XRGs) exhibit two pairs of radio lobes and jets [5], [6]. A recent review [7] summarizes the four different models explaining XRGs: galaxy harbouring twin AGNs, back-flow diversion models, rapid jet reorientation models, finally a new jet-shell interaction model. A large subset of the observations (excepting cases, when the jets are aligned with the optical axes of the host ellipticals [8]) are well-explained by the jet reorientation model, which in turn implies a spin-flip [5], [9] of the dominant black hole.

The details of how this would occur were worked out in Ref. [4]. A key element was the determination of the typical mass ratio at SMBH mergers by a series of estimates, which resulted in mass ratios $\nu = m_2/m_1 = 1/30$ to $\nu = 1/3$. Because the spin scales with the mass squared, the second spin was neglected and only the dominant spin \mathbf{S}_1 (with magnitude S_1) kept. We summarize the consequences of this model as follows.

a) For the typical mass ratio the dominance of L over S_1 is reversed as the separation in the binary decreases throughout the inspiral. In the last stages of the inspiral the spin dominates over the orbital angular momentum $S_1 \gg L$.

b) The angle α between the orbital angular momentum and total angular momentum \mathbf{J} (with magnitude J), also the angle β between the dominant spin and

total angular momentum evolve as:

$$\dot{\alpha} = -\frac{\dot{L}}{J} \sin \alpha > 0 , \quad (1)$$

$$\dot{\beta} = \frac{\dot{L}}{J} \sin \alpha < 0 . \quad (2)$$

c) The approximate expression relating α to the post-Newtonian parameter ε , mass ratio ν and initial angle $\alpha + \beta$ span by the dominant spin with the orbital angular momentum (this angle being a constant during the inspiral) is:

$$\tan \alpha \approx \frac{\sin(\alpha + \beta)}{\varepsilon^{-1/2}\nu + \cos(\alpha + \beta)} . \quad (3)$$

(In Eq. (41) of Ref. [4] the left hand side was given as $\sin 2\alpha / (1 + \cos 2\alpha)$.)

In a criticism to the work presented in Ref. [4], Gopakumar recently argued that "it is unlikely that the spin-flip phenomenon will occur during the binary black hole inspiral phase" [10]. This misconception comes from mixing up the *instantaneous* change in the direction of the total angular momentum, $d\hat{\mathbf{J}}/dt = (\dot{L}/J) [\hat{\mathbf{L}} - (\hat{\mathbf{L}} \cdot \hat{\mathbf{J}}) \hat{\mathbf{J}}] \neq 0$ with its *averaged* expression $\langle d\hat{\mathbf{J}}/dt \rangle = 0$ over the precessional time-scale. The angles α and β are *not* constants during the post-Newtonian evolution, as claimed in Ref. [10], they rather change as given in Eqs. (1)-(2).[‡]

In the present paper we revisit some of the arguments of the spin-flip mechanism and also provide more details on it as compared to Ref [4]. In Section 2 we revisit the typical mass ratio argument, following a recent statistics of supermassive black hole candidates, resulting a newly established mass distribution. We comment on how these findings would affect the typical mass ratio range at SMBH encounters. In Section 3 we analyze how the spin-flip angle depends on the mass ratio and relative orientation of the spin and orbital angular momentum. We also derive a formula for the final spin during the inspiral. Finally we present our Concluding Remarks.

2. The sky in black holes: new statistics, consequences for the mass ratio at SMBH encounters and chances of the spin-flip during the inspiral

First we summarize the arguments of Ref. [4] on the mass ratios at SMBH encounters. The mass distribution $\Phi_{BH}(M_{BH})$ of the galactic central SMBHs in the mass range $3 \times 10^6 \div 3 \times 10^9 M_\odot$ is well described by a power-law with an exponential cutoff, but for our purposes can be adequately approximated by a broken power-law [11]-[13] (confirmed by an observational survey [14]). The break is at about $10^8 M_\odot$. In agreement with these arguments and observations we assume $\Phi_{BH}(M_{BH}) \propto M_{BH}^{-k}$, with $k \in (1, 2)$ below, and $\Phi_{BH}(M_{BH}) \propto M_{BH}^{-h}$, with $h \geq 3$ above the break. Then the probability for a specific mass ratio arose as an integral over the black hole mass distribution, folded with

[‡] Only when the total and orbital angular momenta are aligned, become the angles α and β individually constant, as they identically vanish. Therefore in the aligned configuration no spin-flip could ever occur by the combined mechanism of SO precession and gravitational radiation.

the rate F to merge, and by adopting the lower values of the exponents. For the merger rate we assumed that it scales with the capture cross section S (the dependence on the relative velocity of the two galaxies was neglected, as the universe is not old enough for mass segregation). For the capture cross-section we assumed $S \propto \nu^{-1/2}$, motivated by the following arguments:

- for galaxies an increase with a factor of 10 in radius (10^2 in cross-section) accounts for an increase with a factor of 10^4 in mass (from the comparison of our Galaxy with dwarf spheroidals [15]-[16],
- there is a well established correlation between the SMBH mass and the mass of the host bulge [17],
- the mass of the central SMBH scales with both the spheroidal galaxy mass component and the total, dark matter dominated mass of a galaxy [18].

As a result of these considerations we have found that most likely the mass ratio is in the range $\nu \in (1/30, 1/3)$. A typical value to consider would be $\nu = 1/10$, thus one of the SMBHs being 10 times as massive as the other.

New work on the statistical analysis of 5,895 NED candidate sources [19] has been carried out in the mass range from $10^5 M_\odot$ to above $10^9 M_\odot$. Below about $10^6 M_\odot$ all candidates are probably compact star clusters, however the rest are likely SMBHs. This work shows that the SMBH mass function is a broken power law with M_{BH}^{-2} at low masses, and M_{BH}^{-3} at high masses, with a break near $1.25 \times 10^8 M_\odot$; this general behaviour has been long known, and has now been rederived with a very large sample. The key difference with respect to previous work was the careful attention paid in order to have equal probability for detecting a SMBH in a galaxy, regardless to the Hubble type. The mass distribution of the SMBHs is represented on Fig 1. This particular distribution can be interpreted in the context of the merger model [20] with a merger rate scaling as $(mass)^{+2}$, very much stronger than what we favored in Ref [4]. The extreme mass dependence describes well a M_{BH}^{-3} black hole mass distribution consistent with the high end of the mass distribution; on the other hand a mass dependence of the merger rate close to $(mass)^{+4/3}$, suggested by gravitational focusing arguments [20] describes well the lower mass distribution nearer to M_{BH}^{-2} . It remains to be seen, whether all details of the mass function can be understood using either of these mass ratio dependences. Of course these simple merger rate calculations assume an environment without cosmological expansion. However, for the densest part of the cosmos the local expansion is very weak [21], and that is where most of the mergers occur.

However, for the determination of the typical mass ratio the essential result is only slightly changed. A merger rate running with $mass^{+2}$ analytically gives a M_{BH}^{-3} mass function (see [20]), as observed; we use this rate to estimate here the typical mass ratios for high BH masses. Redoing the integrals of Section 2 of Ref. [4] with $k = 2$, $h = 3$ (denoted there α, β) and $\xi = 2$ (as in [20], so much more extreme than what was assumed in [4]), then all four integrals are still dominated by the lower bound; only the second of the integrals has $q \equiv \nu^{-1}$ in its lower bound, and so the four integrals have the

q -dependencies of q^0 , q^{+1} , q^{-1} and again q^{-1} . We can ignore the second integral, since it all refers to lower masses merging with lower masses. The most important integrals are those combining a SMBH above the break with a SMBH either below or above the break. Then the distribution in q is found as q^{-1} , a logarithmically even distribution in $(dq)/q$ over a range of q from 1 to 1000, so a logarithmic average of 30. Weighting the two parts of the distribution, the larger mass ratios are favored, which would skew the logarithmic average of the mass ratio to $q > 30$, thus $\nu < 0.03$.

The logarithmically even distribution means that the mass ratio ranges ν from 1 to $1/3$, from $1/3$ to $1/10$, from $1/10$ to $1/30$, from $1/30$ to $1/100$, from $1/100$ to $1/300$ and finally from $1/300$ to $1/1000$ are roughly equal likely. A glance at Table 1 of Ref. [4] shows, that concerning the behaviour of the ratio of the dominant spin and orbital angular momentum magnitudes, we have three regimes:

- (1) $\nu \in (1/3, 1)$ when $S_1 < L$ throughout the inspiral,
- (2) $\nu \in (1/30, 1/3)$ when the initial $S_1 < L$ is reversed to $S_1 > L$ during the inspiral and
- (3) $\nu \in (1/1000, 1/30)$ when $S_1 > L$ holds throughout the inspiral.

For the mass ratio ranges (1) and (3) no spin-flip can occur during the inspiral, while for (2) it should. For (1) there is chance for a spin-flip to occur during the plunge, as some numerical simulations have already found this for equal masses [22]. For (3) by contrast there is no possibility for a spin-flip by the combined mechanism of SO precession and gravitational radiation. These mass ratio ranges then occur with (1) 20%, (2) 40% and (3) again 40% probability. This means that *the spin-flip still typically occurs during the inspiral*.

3. Spin-flip angle distribution

In this section we will present an analysis of the spin-flip angle occurring during the inspiral phase in the mass ratio range $\nu \in (1/30, 1/3)$ as a function of the mass ratio.

The spin-flip model be understood as follows. Initially the galactic SMBH has conserved spin, along which the primary jet can form. When the two galaxies collide, the SO induced spin precession starts, while gravitational radiation is diminishing the orbital angular momentum. The direction of the total angular momentum stays unchanged. The constancy of $\hat{\mathbf{J}}$ over the precessional time-scale is due to the fact, that the change in the total angular momentum $\dot{\mathbf{J}} = \dot{L}\hat{\mathbf{L}}$ is about the orbital angular momentum, which (disregarding gravitational radiation) undergoes a precessional motion about \mathbf{J} . This shows that the averaged change in \mathbf{J} is along \mathbf{J} (simple precession, [3]). This conclusion, however, depends strongly on whether the precessional angular frequency Ω_p is larger than $\dot{\alpha}$ and $\dot{\beta}$. Indeed, if these are comparable, the component perpendicular to \mathbf{J} in the change $\dot{\mathbf{J}} = \dot{L}\hat{\mathbf{L}}$ will not average out during one precessional cycle, as due to the increase of α it can significantly differ at the beginning and at the end of the same precessional cycle. Such a situation would occur, when the spin and the orbital angular momentum are of comparable magnitude ($S_1 \approx L$, a regime through which a binary with typical

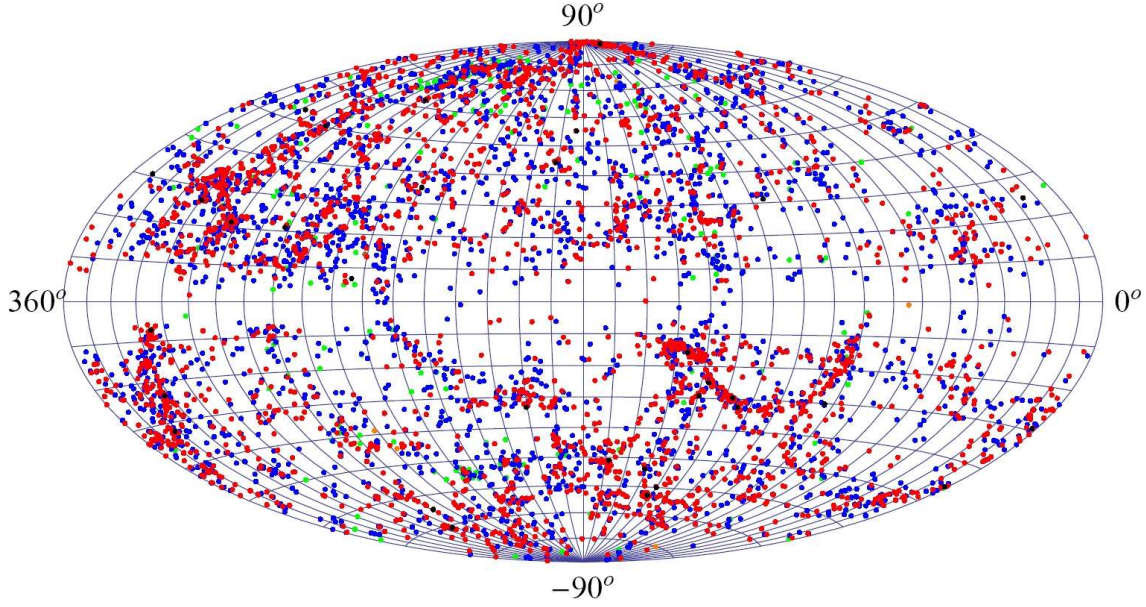


Figure 1. Aitoff projection in galactic coordinates of 5,895 NED SMBH candidate sources. The complete sample is complete in a sensitivity sense, in order to derive densities one needs a volume correction. In the electronic version the colour code is Orange, Green, Blue, Red, Black corresponding to masses above $10^5 M_\odot$, $10^6 M_\odot$, $10^7 M_\odot$, $10^8 M_\odot$, $10^9 M_\odot$, respectively. With the exception of the less numerous first range (Orange), representing compact star clusters, the rest are SMBHs.

mass ratio will pass through during the inspiral) and also roughly antialigned, a low probability regime known as transitional precession. During simple precession Eqs. (1)-(2) governing the evolution of the angles α and β also hold in an average sense over the precessional time-scale. In what follows, we assume simple precession.

The magnitude of the spin is unaffected by gravitational radiation, therefore by the simple rule of addition of vectors the spin has to align close to the $\hat{\mathbf{J}}$ direction. The second jet then can start to form. In the intermediate phase when the spin precesses, instead of jet formation the precessing magnetic field creates a wind, sweeping away the base of the old jet, which in many cases can be observed.

3.1. Spin and orbital angular momentum orientations, final spin formula

The key equation to start with is Eq. (3). In order to see the validity of this equation, also to *generalize* it to the cases of *non-extreme rotation*, we need to evaluate

$$\begin{aligned} S_1 &\approx m_1 R V_1 \approx m_1 \frac{G m_1}{c^2} c \frac{V_1}{c} \approx \frac{G}{c} m_1^2 \chi_1, \\ L &\approx L_N \approx \mu r v = \frac{G}{c} \frac{v}{c} \frac{c^2 r}{G m} \mu m = \frac{G}{c} \varepsilon^{-1/2} m_1 m_2 = \frac{G}{c} m_1^2 (\varepsilon^{-1/2} \nu). \end{aligned} \quad (4)$$

Here V is some characteristic rotational velocity, R the radius of the SMBH (of the order of its Schwarzschild radius) and $\chi_1 \in (0, 1)$ is the dimensionless ($\chi_1 = 1$ for extreme

rotation). Therefore

$$\frac{S_1}{L} \approx \chi_1 \varepsilon^{1/2} \nu^{-1} . \quad (5)$$

Next we express J/S_1 first from $J = L \cos \alpha + S_1 \cos \beta$ by rewriting $\beta = (\alpha + \beta) - \alpha$, and secondly from the equality of the projections perpendicular to $\hat{\mathbf{L}}$ of the total and spin angular momenta $J \sin \alpha = S_1 \sin(\alpha + \beta)$, so that we can equal them. By also employing Eq. (5) and basic trigonometry we obtain

$$\tan \alpha \approx \frac{\sin(\alpha + \beta)}{\chi_1^{-1} \varepsilon^{-1/2} \nu + \cos(\alpha + \beta)} . \quad (6)$$

This is the desired generalization of Eq. (3).

It is worth to note that when applied to the final configuration ε_{fin} , Eq. (6) also stands as a formula for the *final spin at the end of the inspiral*, giving the polar angle of the final spin α_{fin} with respect to the axis $\hat{\mathbf{J}}$ in terms of the mass ratio, spin magnitude and angle span with the orbital angular momentum. Related formulae based on numerical runs were advanced in Refs. [23]. These results are not immediate to compare with ours, as Eq. (6) could at most be applied at the end of the inspiral; although in the mass ratio range where it is valid, one would intuitively expect that as not much orbital angular momentum is left at the end of the inspiral in comparison with the dominant spin, the direction of the latter will not be significantly changed during the plunge.

3.1.1. Particular cases. There are three particular configurations worth to mention:

i) The spin is aligned with the orbital angular momentum: $\alpha + \beta = 0$, thus from Eq. (6) $\alpha = 0$ and there is no room for any spin-flip. This would be the situation for perfectly wet mergers, which align the spin with the orbital angular momentum.

ii) The spin is anti-aligned with the orbital angular momentum, $\alpha + \beta = \pi$. Therefore depending on which of the S_1 and L are larger, the angle α is either 0 or π .

iii) For the parameter ranges when the denominator vanishes $\alpha + \beta = \arccos(-\chi_1^{-1} \varepsilon^{-1/2} \nu)$, from Eq. (6) we obtain $\alpha = \pi/2$, therefore β is also determined.

3.1.2. Discussion as function of mass ratios. Keeping in mind that due to Eqs. (1)-(2) the angle $\alpha + \beta$ is a constant during the inspiral (a parameter), and the dimensionless spin χ_1 behaves similarly, also regarding the mass ratio as a third parameter characterizing the particular merger, the angle α in general remains a function of ε , thus it evolves together with the orbital separation r and velocity v .

For the mass ratio $\nu = 1/10$ we have $(S_1/L)_{in} \approx \chi_1 \varepsilon_{in}^{1/2} \nu^{-1} = 0.316 \chi_1$ and $(S_1/L)_{fin} \approx \chi_1 \varepsilon_{fin}^{1/2} \nu^{-1} = 3.162 \chi_1$. As $\tan \alpha \leq S_1/L$ and $\tan \beta \leq L/S_1$ (the equalities arising when the spin and orbital angular momentum are perpendicular) we have $\tan \alpha_{in} \leq 0.316 \chi_1$ and $\tan \beta_{fin} \leq 0.316 \chi_1^{-1}$. For extreme rotation ($\chi_1 = 1$) we obtain $\alpha_{in}, \beta_{fin} \leq 0.316 = 18.105^\circ$.

For $\nu = 1/3$ we obtain $\tan \alpha_{in} \leq (S_1/L)_{in} \approx \chi_1 \varepsilon_{in}^{1/2} \nu^{-1} = 0.095 \chi_1$ and for extreme rotation $\alpha_{in} \leq 0.095 = 5.44^\circ$. In fact at the beginning of the inspiral this latter condition (meaning that the orbital angular momentum is roughly the total angular momentum) holds in the whole mass ratio range $\nu \in (1/3, 1)$. Under these conditions Eq. (6) can be approximated as

$$\alpha_{in} \approx \chi_1 \varepsilon_{in}^{1/2} \nu^{-1} \sin \beta_{in} = 0.032 \chi_1 \nu^{-1} \sin \beta_{in} . \quad (7)$$

For $\nu = 1/30$ we obtain $\tan \beta_{fin} \leq (L/S_1)_{fin} \approx \chi_1^{-1} \varepsilon_{fin}^{-1/2} \nu = 0.105 \chi_1^{-1}$ and for extreme rotation $\beta_{fin} \leq 0.105 = 6.04^\circ$. In fact at the beginning of the inspiral this latter condition (meaning that the dominant spin is roughly the total angular momentum) holds in the whole range $\nu \in (1/1000, 1/30)$. Under these conditions Eq. (6) can be expanded (to first order in β_{fin} , with $\chi_1^{-1} \varepsilon_{fin}^{-1/2} \nu$ of the order of β) as

$$\beta_{fin} \approx \chi_1^{-1} \varepsilon_{fin}^{-1/2} \nu \sin \alpha_{fin} = 3.162 \chi_1^{-1} \nu \sin \alpha_{fin} . \quad (8)$$

For slowly rotating SMBHs with $\chi_1 \approx 0.1$ the above formula would hold only in the range $\nu \in (1/1000, 1/300)$.

3.2. The spin-flip angle during the inspiral

A minimal value for the spin-flip angle σ arises by forming the difference between the angles β , characterizing the orientation of the spin with respect to the inertial direction $\hat{\mathbf{J}}$. Thus

$$\sigma_{\min} = \beta_{in} - \beta_{fin} = \alpha_{fin} - \alpha_{in} . \quad (9)$$

In the second equality we have used that $\alpha_{in} + \beta_{in} = \alpha_{fin} + \beta_{fin}$.

However we have to take into account, that the above is only true in a 2-dimensional picture. In reality the 3-dimensional SO precession will complicate the situation, and the above angle emerges only if the number of precessions during the inspiral is an integer multiple of 2π . If instead is of the type $(2k+1)\pi$ the spin-flip angle will be maximal, to be calculated as

$$\sigma_{\max} = \beta_{in} + \beta_{fin} - l\pi = 2(\alpha_{in} + \beta_{in}) - l\pi - (\alpha_{in} + \alpha_{fin}) , \quad (10)$$

where $l = 0$ if $\beta_{in} + \beta_{fin} \leq \pi$ and $l = 1$ if $\pi < \beta_{in} + \beta_{fin} < 2\pi$.

The difference between σ_{\max} and σ_{\min} is due to the fact, that the realignment of the spin along $\hat{\mathbf{J}}$ is not perfect. The closer \mathbf{S}_1^{fin} is to $\hat{\mathbf{J}}$, the less their difference ought to be due a more perfect alignment, therefore $\sigma_{\max} - \sigma_{\min} = \beta_{fin} - \beta_{in}$ should go to 0 with decreasing ν .

For generic mass ratios $\nu \in (1/30, 1/3)$, Eqs. (6), (9) and (10) give the range of allowed spin-flip angle for each relative orientation $\alpha + \beta$ of the spin with respect to the plane of motion and each χ_1 . The generic numerical solution for σ_{\min} in the case $\chi_1 = 1$ is represented on Fig 2 as function of the relative orientation of the spin and orbital angular momentum $\alpha + \beta$ and mass ratio ν . For a given mass ratio the spin-flip angle has a maximum shifted from $\pi/2$ towards the anti-aligned configurations. The figure

confirms the prediction, that significant spin-flip will occur during the inspiral in the mass ratio range $\nu \in (1/30, 1/3)$. For mass ratios smaller than $1/100$ the spin does not flip at all, as the infalling SMBH acts as a test particle.

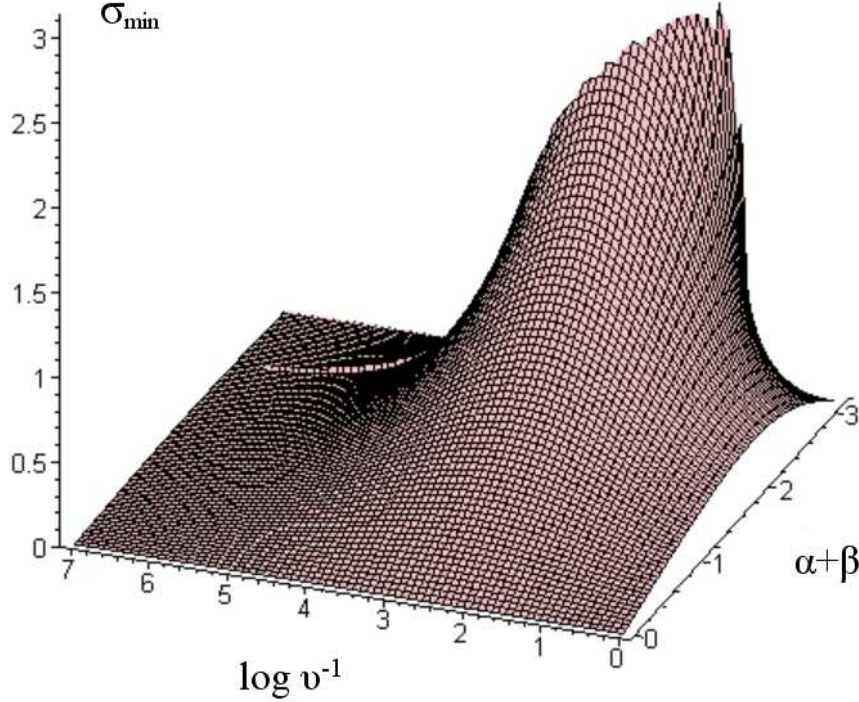


Figure 2. The spin-flip angle σ_{\min} as function of the relative orientation of the spin and orbital angular momentum $\alpha + \beta$ (a constant during inspiral), and mass ratio ν . For a given mass ratio the spin-flip angle has a maximum shifted from $\pi/2$ towards the anti-aligned configurations. The mass ratios $\nu = 1$; $1/3$; $1/30$ and $1/1000$ are located on the $\log \nu^{-1}$ axis at 0; 1.09; 3.40 and 6.91, respectively, confirming the prediction, that a significant spin-flip will occur in the mass ratio range $\nu \in (1/30, 1/3)$. For mass ratios smaller than $1/100$ the spin does not flip at all, as the infalling SMBH acts as a test particle.

4. Concluding Remarks

In light of the new data on a large sample of SMBH candidates we have established that the mass ratios obey an even logarithmic distribution in ν . In the mass ratio range $\nu \in (1/30, 1/3)$ of SMBH mergers representing 40% of all possible cases, we have investigated the SO precession driven conservative and gravitational radiation driven dissipative contributions to the orbital evolution during the inspiral, averaged over the precession time-scale. In this mass range the ratio of the dominant spin magnitude and orbital angular momentum magnitude S/L changes from *less than 1* to *larger than 1* during the inspiral. As the direction of the total angular momentum is unchanged on all

time-scales larger than the precession time-scale, while the magnitude of the the orbital angular momentum decreases due to gravitational radiation and the magnitude of the spin stays constant, the spin direction has to change. The spin-flip of the dominant spin therefore occurs during the *inspiral*. If jet activity is involved, X-shaped radio galaxies arise by this mechanism and a large set of observations on X-shaped radio galaxies could be explained.

In another 40% of the mergers with mass ratios $\nu \in (1/1000, 1/30)$ the spin-flip never occurs by this mechanism, while in the remaining 20% of mergers with mass ratios $\nu \in (1/3, 1)$ it may occur during the plunge.

SMBH mergers of equal mass to $\nu = 1/3$ are only half as likely as the mass ratios $1/30$ to $1/3$, therefore the occurrence of the spin-flip can be considered typical during the inspiral. We analyzed the magnitude of the spin-flip angle occurring during the inspiral as function of the mass ratio and original relative orientation of the spin and orbital angular momentum and supported by numerical analysis the theoretical prediction (Fig 2). We also derived a formula for the *final spin* at the end of the inspiral in this mass ratio range.

During the inspiral the following relations among the relevant time-scales hold: tilt / spin-flip time-scale \geq inspiral time-scale \gg precession time-scale \gg orbital time-scale (for all mass ratios in the typical range). Interestingly enough, the spin-flip time-scale for a typical mass ratio of $1/10$ is only about three years, while the precession time-scale is less then a day [4]. Thus rapidly rotating relativistic jets coming close to our line of sight could produce significant variability at all wavelengths years before the coalescence. Therefore electromagnetic counterparts / precursors to the strongest gravitational wave emission are also likely to occur.

Acknowledgements

This work was supported by the Polányi Program of the Hungarian National Office for Research and Technology (NKTH), the Hungarian Scientific Research Fund (OTKA) grant 69036 and the COST Action MP0905 (LÁG); AUGER membership and theory grant 05 CU 5PD 1/2 via DESY/BMBF and VIHOS (PLB); and contracts CNCSIS 539/2009 and CNMP 82077/2008 (LIC).

References

- [1] K. G. Arun, S. Babak, E. Berti, N. Cornish, C. Cutler, J. Gair, S. A. Hughes, B. R. Iyer, R. N. Lang, I. Mandel, E. K. Porter, B. S. Sathyaprakash, S. Sinha, A. M. Sintes, M. Trias, C. Van Den Broeck, M. Volonteri, *Class. Quantum Grav.* **26**, 094027 (2009); R. N. Lang, S. A. Hughes, *Class. Quantum Grav.* **26**, 094035 (2009).
- [2] B. M. Barker and R. F. O’Connell, *Phys. Rev. D* **12**, 329 (1975); B. M. Barker and R. F. O’Connell, *Gen. Rel. Grav.* **11**, 149 (1979); L. E. Kidder, C. M. Will, A. G. Wiseman, *Phys. Rev. D* **47**, R4183 (1993); L. E. Kidder, *Phys. Rev. D* **52**, 821 (1995); F. D. Ryan, *Phys. Rev. D* **53**, 3064 (1996); R. Rieth, G. Schäfer, *Class. Quantum Grav.* **14**, 2357 (1997); L. Á. Gergely, Z. Perjés, M. Vasúth, *Phys. Rev. D* **57**, 876 (1998); L. Á. Gergely, Z. Perjés, M. Vasúth, *Phys. Rev. D*

- 57**, 3423 (1998); L. Á. Gergely, Z. I. Perjés, M. Vasúth, *Phys. Rev. D* **58**, 124001 (1998); R. F. O’Connell, *Phys. Rev. Letters* **93**, 081103 (2004); C. M. Will, *Phys. Rev. D* **71**, 084027 (2005); M. Campanelli, C. O. Lousto, Y. Zlochower, *Phys. Rev. D* **74**, 084023 (2006); J. Zeng, C. M. Will, *Gen. Rel. Grav.* **39** 1661-1673 (2007); J. Majár, M. Vasúth, *Phys. Rev. D* **77**, 104005 (2008); N. J. Cornish, J. Shapiro Key, *Computing waveforms for spinning compact binaries in quasi-eccentric orbits*, arXiv:10045322 (2010).
- [3] T. A. Apostolatos, C. Cutler, G. J. Sussman, K. S. Thorne, *Phys. Rev. D* **49**, 6274 (1994).
- [4] L. Á. Gergely, P. L. Biermann, *Astrophys. J.* **697**, 1621 (2009).
- [5] J. P. Leahy, A. G. Williams, *Mon. Not. Royal. Astron. Soc.* **210**, 929 (1984).
- [6] J. P. Leahy, R. A. Perley, *Astron. J* **102**, 537 (1991); A. R. S. Black, S. A. Baum, J. P. Leahy, R. A. Perley, J. M. Riley, P. A. G. Scheuer, *Mon. Not. Royal. Astron. Soc.* **256**, 186 (1992).
- [7] Gopal-Krishna, P. L. Biermann, L. Á. Gergely, P. J. Wiita, *On the origin of X-shaped radio galaxies*, *New Astron. Rev.* (to appear).
- [8] R. A. Battye, I. W. A. Browne, *Mon. Not. Royal Astron. Soc.* **399**, 1888 (2009).
- [9] Ch. Zier, P. L. Biermann, *Astron. Astroph.* **377**, 23 (2001); D. Merritt, R. Ekers, *Science* **297**, 1310 (2002); Gopal-Krishna, P. L. Biermann, P. J. Wiita, *Astrophys. J. Letters* **594**, L103 (2003); F. K. Liu, *Mon. Not. Royal. Astron. Soc.* **347**, 1357 (2004).
- [10] A. Gopakumar, invited and highlight talk presented at the *Workshop on Massive Black Hole Binaries and Their Coalescence in Galactic Nuclei*, KIAA, Peking University, Beijing July 20-25, 2009, <http://vega.bac.pku.edu.cn/~fkliu/binary09/pdf/Gopakumar.pdf>
- [11] W. H. Press, P. Schechter, *Astrophys. J.* **187**, 425 (1974)
- [12] A. S. Wilson, E. J. M. Colbert, *Astrophys. J.* **438**, 62 (1995)
- [13] T. R. Lauer et al., *Astrophys. J.* **662**, 808L (2007)
- [14] L. Ferrarese et al., *Astrophys. J. Suppl. Ser.* **164**, 334 (2006)
- [15] G. Gilmore et al., *Nucl. Phys. B* **173**, 15 (2007)
- [16] A. Klypin, H.-S. Zhao, R. S. Somerville, *Astrophys. J.* **573**, 597 (2002)
- [17] J. Magorrian et al., *Astronomical J.* **115**, 2285 (1998)
- [18] A. J. Benson, D. Džanović, C. S. Frenk, R. Sharples, *Mon. Not. Roy. Astron. Soc.* **379**, 841 (2007)
- [19] L. I. Caramete, P. L. Biermann, *The mass function of nearby black hole candidates*, to appear in *Astron. Astroph.* (2009), E-print: arXiv:0908.2764
- [20] J. Silk, T. Takahashi, *Astrophys. J.* **229**, 242 (1979)
- [21] A. Cavaliere, S. Colafrancesco, N. Menci, *Astrophys. J.* **392**, 41 (1992)
- [22] M. Campanelli, C. O. Lousto, Y. Zlochower, B. Krishnan, D. Merritt, *Phys. Rev. D* **75** 064030 (2007)
- [23] L. Rezzolla, E. Barausse, E. Nils Dorband, D. Pollney, C. Reisswig, J. Seiler, S. Husa, *Phys. Rev. D* **78** 044002 (2008); M. C. Washik, J. Healy, F. Herrmann, I. Hinder, D. M. Shoemaker, P. Laguna, R. A. Matzner, *Phys. Rev. Lett.* **101** 061102 (2008); A. Buonanno, L. E. Kidder, L. Lehner, *Phys. Rev. D* **77** 026004 (2008); W. Tichy, P. Marronetti, *Phys. Rev. D* **78**, 081501(R) (2008); E. Barausse, L. Rezzolla, *Astrophys. J. Lett.* **704** L40-L44 (2009); U. Sperhake, V. Cardoso, F. Pretorius, E. Berti, T. Hinderer, N. Yunes, *Phys. Rev. Lett.* **103**, 131102 (2009); J. Healy, P. Laguna, R. A. Matzner, D. M. Shoemaker, *Phys. Rev. D* **81**, 081501 (2010); E. Barausse, *The importance of precession in modelling the direction of the final spin from a black-hole merger*, E-print: arXiv:0911.1274 (2009); M. Kesden, U. Sperhake, E. Berti, *Phys. Rev. D* **81**, 084054 (2010); C. O. Lousto, H. Nakano, Y. Zlochower and M. Campanelli, *Phys. Rev. D* **81**, 084023 (2010); C. O. Lousto, M. Campanelli, Y. Zlochower, H. Nakano, *Class. Quantum Grav.* **27**, 114006 (2010)